Talanta 85 (2011) 1050–1055

Contents lists available at ScienceDirect

Talanta

journal homepage: www.elsevier.com/locate/talanta

Ferrocene based chemosensor for Cu^{2+}—A dual channel signaling system

Paramjit Kaur[a,*], Mandeep Kaur[a,b], Kamaljit Singh[b,*]

[a] Department of Chemistry, Guru Nanak Dev University, Amritsar 143005, India
[b] Organic Synthesis Laboratory, Department of Applied Chemical Sciences and Technology, Guru Nanak Dev University, Amritsar 143005, India

ARTICLE INFO

Article history:
Received 21 March 2011
Received in revised form 7 May 2011
Accepted 12 May 2011
Available online 20 May 2011

Keywords:
Ferrocene
Dual channel
Chemosensor
Absorption
Electrochemical

ABSTRACT

A new ferrocene based molecule behaves as a dual channel signaling chemosensor for Cu^{2+} over other metal ions. The perturbations in the absorption pattern and electrochemical behavior of the chemosensor are presented. These have been proposed to be caused by the interaction of Cu^{2+} with the d-electrons and the electron rich π-system of the ferrocenyl derivative. The sensing event is manifested by a high energy shift in the ligand centered π–π^* absorption and appearance of a new redox wave at more positive potential, in addition to Fe(II)/Fe(III) couple wave (two wave electrochemical behavior).

1. Introduction

Copper is one of the heavy metals which is beneficial not only for human beings but for plants also [1]. At the same time, its widespread use for industrial, pharmaceutical and agricultural purposes is accompanied by a serious threat to the environment [2] which is attributed to its ionic form, Cu^{2+}. This veracity of its beneficial as well as harmful effects has aroused considerable interest in the development of probes for selective sensing of Cu^{2+}. Although a number of single-signaling: absorption, emission [3] and redox [4] based chemosensors for Cu^{2+} have been designed and synthesized in the recent years, there is a dearth of multichannel signaling receptors reporting the presence of Cu^{2+} via multiple signaling patterns, especially absorption/redox and emission/redox based changes. On the other hand, literature reports [5] indicate that ferrocene has proved to be a simple building block for the preparation of derivatives which can be explored for the redox based sensing of analytes. Further, the presence of analytes perturb the redox couple Fe(II)/Fe(III) as well as the characteristic absorption bands of ferrocene derivatives [6]. These types of probes contain ferrocene units and nitrogen/oxygen donor complexing moieties. There are number of reports on such systems which are well addressed by Molina et al. in their review [7]. If the ferrocene derivatives contain fluorescent moieties, they may act as dual, fluorescent-electrochemical chemosensors for which there are limited reports, probably ferrocene residues act as quenchers for the fluorescent unit through the electron transfer mechanism [8]. Thus, it is evident from the literature reports that the ferrocene based systems may act as multichannel chemosensors if they possess complexing and/or fluorescent moieties by allowing their redox behavior to couple with optical behavior. In continuation of the interest of our research group [9] in developing chemosensors for guest ions, in the present investigation, we report design of a ferrocene derivative **2** (Scheme 1), which neither contains efficient complexing unit for cations nor a fluorescent unit, but acts as a highly selective dual channel chemosensor for Cu^{2+}. To explain the sensing event, a mechanism based upon the interaction of Cu^{2+} with π electrons of the chromophore and the d-electrons of the ferrocene unit, has been proposed.

2. Experimental

2.1. Chemicals

Metal salts used in the spectrophotometric studies were of analytical grade and bought from Sigma–Aldrich. For the titrations, Li^+, Na^+, Mg^{2+}, Ca^{2+}, Ba^{2+}, Cr^{3+}, Mn^{2+}, Co^{2+}, Ni^{2+}, Hg^{2+}, Pb^{2+}, Cu^{2+} were added as their perchlorates and K^+, Zn^{2+}, Cd^{2+}, Ag^+, La^{3+}, Ce^{3+}, Pr^{3+}, Nd^{3+}, Sm^{3+}, Eu^{3+}, Gd^{3+}, Tb^{3+}, Yb^{3+}, Lu^{3+}, NH_4^+ were added as their nitrates. The solvents used were of analytical grade and purchased from Thomas Baker.

2.2. Instrumentation

Mass spectrum was recorded on Bruker Daltonics esquire 3000 spectrometer. ^1H NMR and ^{13}C NMR spectra were recorded in $CDCl_3$ on BRUKER AVANCE II at 400 and 100 MHz, and JEOL-FT NMR-AL

---

[*] Corresponding authors.
E-mail addresses: paramjit19in@yahoo.co.in (P. Kaur), kamaljit19in@yahoo.co.in (K. Singh).

0039-9140/$ – see front matter © 2011 Elsevier B.V. All rights reserved.
doi:10.1016/j.talanta.2011.05.026

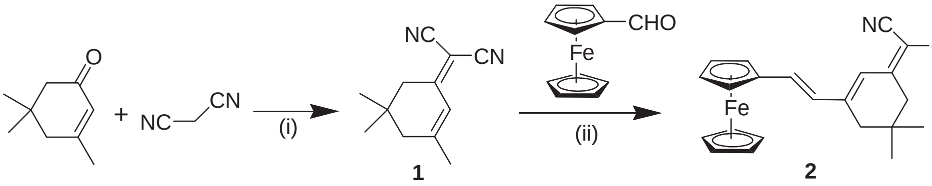

(i) DMF, AcOH, Ac_2O, piperidine, 120°C, 6h (ii) CH_3CN, piperidine, 80°C, 4h

Scheme 1. Synthesis of **2**.

at 300 and 75 MHz respectively, using TMS as an internal standard. Data are reported as follows: chemical shift in ppm (δ), integration, multiplicity (s = singlet, d = doublet), coupling constant J (Hz) and assignment. IR spectrum was recorded on Varian 660-IR Fourier-Transform spectrophotometer in the range 400–4000 cm^{-1} using KBr as medium. The purity of the solid products was checked by elemental analysis performed on Thermoelectron FLASH EA1112 CHNS analyzer. UV–visible spectral studies were conducted on SHIMADZU 1601 PC spectrophotometer with a quartz cuvette (path length, 1 cm). The cell holder of the spectrophotometer was maintained at 25 °C for consistency in the recordings. The absorption spectra were recorded between 1100 and 200 nm. The pH titrations were performed with the Equip-Tronics Digital pH meter model-EQ 610. Electrochemical studies were carried out on CHI 660C Electrochemical Workstation with a conventional three-electrode configuration consisting of platinum working (2 mm diameter) and counter electrodes and Ag/AgCl as reference electrode. The reversibility and the redox behavior of ferrocene/ferrocenium redox couple were determined by cyclic voltammetry and Osteryoung square-wave voltammetry. The experiments were carried out in a 10^{-3} M solution of sample in CH_3CN containing 0.1 M tetrabutylammonium perchlorate (TBAP) as supporting electrolyte at room temperature. Deoxygenation of the solutions was achieved by bubbling nitrogen for 10 min and the working electrode was cleaned after each run. The voltammograms were recorded with a scan rate of 100 mV s^{-1}. The cations were added as a 0.1 M stock solution in water. All the potential values were determined relative to decamethylferrocene. The redox behavior of the compound was observed to be reversible as, (i) separation between the cathodic and anodic peak is 77 mV, (ii) peak potential does not changes on changing sweep rate, and (iii) the ratio between the cathodic and anodic current is close to unity.

2.3. *Procedure for synthesis of **2** (Scheme 1)*

2.3.1. *Synthesis and characterization of 2-(3,5,5-trimethylcyclohex-2-enylidene)malononitrile, **1** (Scheme 1)*

The compound **1** was prepared according to the literature report [10] (S1, See the Supporting Information).

2.3.2. *Synthesis and characterization of (E)-2-[(3-(2-ferrocenyl)vinyl)-5,5-dimethylcyclohex-2-enylidene]malononitrile, **2***

To a mixture of compound **1** (0.432 g, 3.0 mmol) and piperidine (catalytic amount, 2 drops) in dry CH_3CN (40 mL) ferrocene carboxaldehyde (0.214 g, 1.0 mmol) was added. The mixture was refluxed at 80 °C for 4 h. The separated solid was filtered and purified by column chromatography on silica gel (60–120 mesh) using hexane/ethyl acetate mixtures as the eluent. The compound was recrystallized in hexane/dichloromethane. Green solid. Yield 75%. Mp: 172 °C. (Found: C, 71.8; H, 5.38; N, 7.21 $C_{23}H_{22}FeN_2$ requires C, 72.2; H, 5.75; N, 7.32%); ν_{max}/cm^{-1}: 3092 (aromatic C–H), 2938.145 (aliphatic C–H), 2204.957 (CN), 1612 (C=C), 1115 (C_5H_5); ^1H NMR (400 MHz): δ 1.07 (6H, s, CH_3), 2.40 (2H, s, CH_2), 2.57 (2H, s, CH_2), 4.15 (5H, s, Cp*H*), 4.48 (2H, d, J = 1.68 Hz, Cp*H*), 4.51 (2H, d, J = 1.68 Hz, Cp*H*), 6.58 (1H, d, J = 15.88 Hz, C=C*H*), 6.72 (1H, s, C*H*), 6.95 (1H, d, J = 15.88 Hz C=C*H*); ^{13}C NMR (100 MHz): δ 28.04, 31.99, 39.16, 42.97, 68.29, 69.86, 71.27, 76.40, 80.84, 113.40, 114.17, 121.12, 126.52, 138.90, 154.35, 169.57; ^{13}C DEPT 135 (100 MHz): 28.04, 39.16 (−ve), 42.97 (−ve), 68.29, 69.86, 71.27, 121.12, 126.52, 138.91; m/z (EI): 381.9 (M^+).

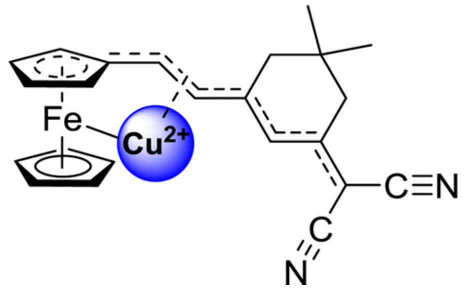

Scheme 2. Proposed binding mode of Cu^{2+} with **2**.

(For copies of the NMR, EI Mass, see S2 in Supporting Information).

2.4. *Isolation of copper complex of **2** (Scheme 2)*

The copper complex of **2** was synthesized by mixing **2** (0.500 g, 1.30 mmol) and $Cu(NO_3)_2 \cdot 3H_2O$ (0.456 g, 1.96 mmol), dissolved in acetonitrile, and stirring the mixture for an hour at room temperature. The solvent was removed under reduced pressure and the solid complex was washed with ethanol and dried. Yield: 80%; Mp: >300 °C; ν_{max}/cm^{-1}: 2923.526 (aromatic CH), 2222.614 (CN), 1616.828 (C=C), 1097.345 (NO).

3. Results and discussion

3.1. *Synthesis*

Scheme 1 shows the synthesis of **2** by the reaction of 1-formylferrocene with **1** prepared from isophorone following a reported method [10]. **2** was isolated as a stable solid in 75% yield and characterized using spectroscopic (S2 in Supporting Information) and microanalytical data.

3.2. *UV–vis studies*

The cation sensing properties of **2** were studied both by optical and electrochemical analyses. The UV–vis absorbance spectrum of **2** in CH_3CN (2.8×10^{-5} M) exhibits two charge-transfer (CT) bands in the region 350–600 nm, characteristic of ferrocenyl chromophores [11]. The high energy band at 406 nm (ε_{max} 32685.12 L mol^{-1} cm^{-1}) is attributed to π–π^* and L–π^* electronic transitions, while a low energy band at 557 nm (ε_{max} 8837.37 L mol^{-1} cm^{-1}) is attributed to Fe (II) d–d transition or metal → ligand CT transition (MLCT) (dπ–π^*) [12] (Fig. 1).

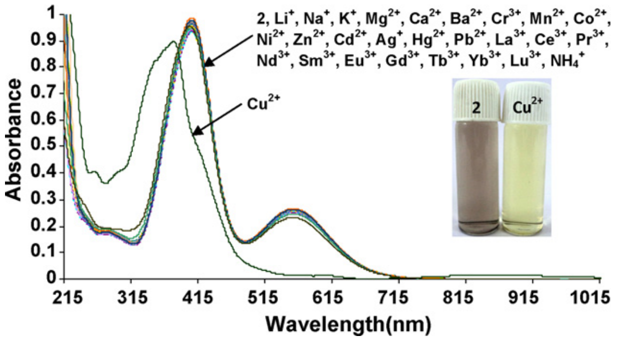

Fig. 1. Changes in the absorption spectrum of **2** (2.8×10^{-5} M, in CH_3CN) upon addition of aqueous solutions of Cu^{2+} (4.2×10^{-5} M) and other metal ions (8.4×10^{-5} M), recorded immediately after mixing. Inset: Colour CHANGE of **2** after addition of Cu^{2+}.

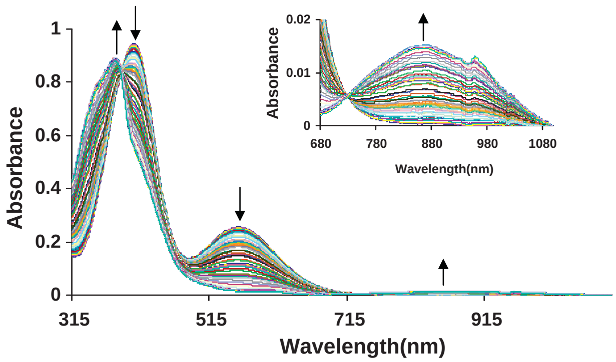

Fig. 3. Changes in the absorption spectrum of **2** (2.8×10^{-5} M, in CH_3CN) upon titration with aqueous solution of Cu^{2+} (5.7×10^{-7} to 8.57×10^{-5} M, in water). Inset: changes in the absorbance of **2** at 871 nm as a function of Cu^{2+} concentration.

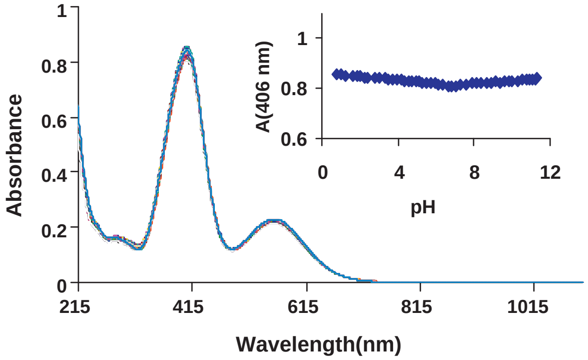

Fig. 2. Changes in the absorbance of **2** upon pH titration with HCl (0.01 M) and NaOH (0.01 M). Inset: changes in the UV–vis spectrum of **2** at 406 nm upon pH titration.

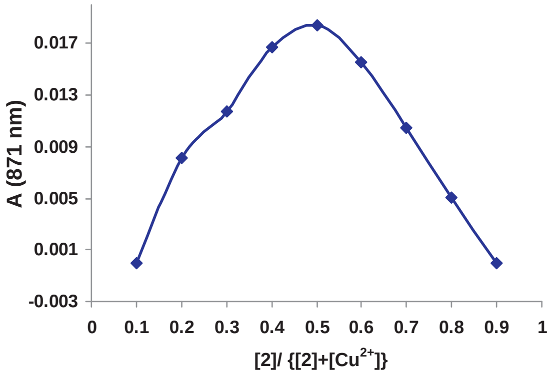

Fig. 4. Job's plot of **2** with Cu^{2+}.

Before investigating the chemosensing properties of **2**, the effect of pH variation on **2** was noted during titration of a 2.8×10^{-5} M solution of **2** with 0.01 M NaOH and HCl. No significant change (Fig. 2) was observed in the wavelength position of the CT absorption bands as well as in the color of **2**, over the covered pH range (2.0–12.0). Thus, **2** demonstrated considerable stability to pH variation which is often considered an advantage for rapid monitoring of aqueous analytes in environmental or biological settings without resorting to buffered media. The UV–vis binding interaction studies of **2** in CH_3CN (2.8×10^{-5} M) exhibit excellent selectivity for Cu^{2+} ions over alkali and alkaline-earth metal ions (Li^+, Na^+, K^+, Mg^{2+}, Ba^{2+}), transition metal ions (Cr^{3+}, Mn^{2+}, Co^{2+}, Ni^{2+}, Zn^{2+}, Cd^{2+}, Ag^+), lanthanides (La^{3+}, Ce^{3+}, Pr^{3+}, Nd^{3+}, Sm^{3+}, Eu^{3+}, Gd^{3+}, Tb^{3+}, Yb^{3+}, Lu^{3+}) (Fig. 1) and the major interferring heavy metal ions in the real life samples (Pb^{2+}, Hg^{2+}). On stepwise addition of Cu^{2+} ions in H_2O (5.7×10^{-7} to 8.57×10^{-5} M) to a solution of **2** in CH_3CN (2.8×10^{-5} M, after mixing the CH_3CN/H_2O ratio was 9:1), the low energy band of **2** disappeared accompanied by a hypsochromic shift of 27 nm in the high-energy band at 406 nm and appearance of a new band at 871 nm. These changes were observed to their maximum when the addition of 4.2×10^{-5} M solution of Cu^{2+} ions was attained, after which no significant change was observed. This perturbation in the absorption spectrum is well appreciated by 'naked-eye' inspection (Fig. S3, see the Supporting Information). The appearance of a low energy band at 871 nm suggests the oxidation of ferrocene moiety to ferrocenium ion in the presence of Cu^{2+}, as documented in the literature [13]. Two well defined isosbestic points were observed at 386 and 735 nm during titrations, supporting the formation of spectrally distinct complex as described above (Fig. 3).

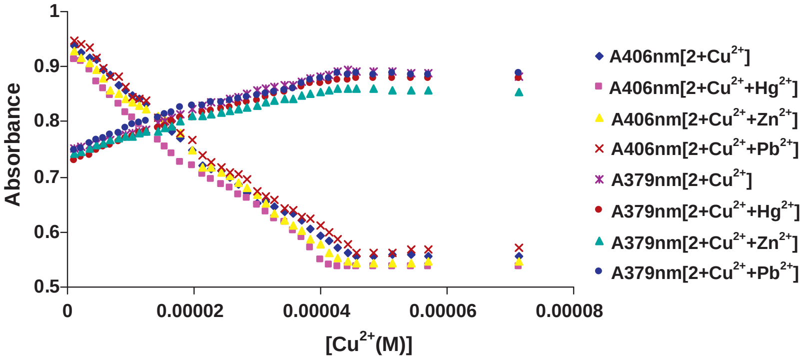

Fig. 5. Changes in the absorption spectrum of **2** (2.8×10^{-5} M, in CH_3CN) upon titration with increasing amount of aqueous solution of Cu^{2+} (5.7×10^{-7} to 8.57×10^{-5} M, in water) in the presence of other metal ions (8.4×10^{-5} M, in water).

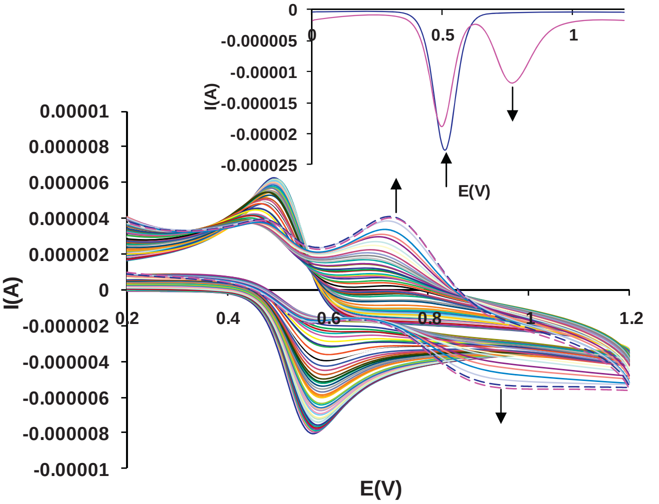

Fig. 6. Changes in the redox properties of **2** (1.0×10^{-3} M, in CH_3CN) upon addition of 1.0 eq. of aqueous solution of Cu^{2+} (1.5×10^{-5} to 1.0×10^{-3} M, in water). Inset: Osteryoung square-wave voltammetry of **2** upon addition of 1.0 eq. of aqueous Cu^{2+} solution.

Titration data of **2** with Cu^{2+} was fitted using HypSpec- a non-linear least-squares fitting programme [14]. It allowed the establishment of the stoichiometry (1:1) of the most stable species (**2**:Cu^{2+}) present in the solution with a binding constant $\log \beta_{1,1} = 4.99$. The 1:1 stoichiometry was further confirmed by using the method of continuous variations (Job's plot), where the absorbance at 871 nm got to maximum when molar fraction of Cu^{2+} was 0.5 (Fig. 4). The detection limit (DL) was found to be 4.93×10^{-6} M [15].

To further evaluate the practical utility of **2** as a Cu^{2+} selective sensor, competitive experiments were carried out especially in the presence of common interfering metal ions such as Hg^{2+}, Zn^{2+} and Pb^{2+}. Thus, when a solution of **2** in CH_3CN (2.8×10^{-5} M) was titrated with Cu^{2+} solution in the presence of Hg^{2+}, Zn^{2+} and Pb^{2+} ions in water (8.4×10^{-5} M), no interference in the detection of Cu^{2+} was noticed (Fig. 5). The preference of **2** for Cu^{2+} is attributed to the presence of partially filled d-orbital in Cu^{2+} to accept the electron lost during oxidation of Fe(II).

3.3. Electrochemical studies

The electrochemical properties of **2** in CH_3CN (1×10^{-3} M) containing 0.1 M [n-Bu_4N]ClO_4 (TBAP) as supporting electrolyte, and its sensing behavior towards different metal ions was investigated using cyclic voltammetric (CV) and Osteryoung square-wave voltammetric (OSWV) techniques. In the cyclic voltammogram of **2**, the expected one-electron reversible oxidation peak attributed to Fe(II)/Fe(III) couple was observed at half-wave potential, $E_{1/2} = 533$ mV. This increased value, in comparison to the ferrocene ($E_{1/2} = 500$ mV) indicates that **2** is more difficult to oxidize [16] which may be due to electron withdrawing power of the dicyanovinyl group, resulting in an increased +ve charge on the iron atom. Addition of 0–1 equivalent of Cu^{2+} ions perturb the formal potential of Fe(II)/Fe(III) couple in terms of diminished current intensity accompanied by the formation of a new redox wave at more positive potential $E_{1/2} = 816$ mV (Fig. 6), attributed to the formation of a complex species of **2** with Cu^{2+} ion. Thus, in the sensing of Cu^{2+}, distinct two wave "electrochemical behavior" of **2**, compared to only single reversible wave (due to Fe(II)/Fe(III) couple) with other analysed cations was observed (Fig. S4, See the supporting information).

The possible mechanism involved in the UV–vis and electrochemical changes in **2** upon sensing of Cu^{2+} may be understood as: in the complexation of the ferrocene derivatives, devoid of any specific ligating sites for cations, either the d-electrons of ferrocene may serve as donors (itself undergoing Fe(II) → Fe(III) change), resulting the close proximity of the cation to the ferrocene unit via orbital-orbital interaction between the cation and the ferrocene d-electrons [17], or in the sufficiently flexible systems such as the conjugated ferrocenyl derivatives, the π-system of the ferrocene [18] and/or the conjugated bridge may act as a donor group for the cation, forming a π-complex, a term normally associated with transition metal and the π-electron rich system interactions [19]. In the former case, the UV–vis spectrum of the ferrocenyl derivative in the presence of cation is not expected to show Fe(II) d-d transition, normally observed as a medium intensity low energy band at 500–600 nm, rather will exhibit a band at 750–850 nm attributed to the formation of ferrocenium ion. While in the latter, a hypsochromic shift in the characteristic $\pi \rightarrow \pi^*$ electronic transition of the conjugated ferrocenyl derivative, due to reduced participation of π-electrons in the electron transfer process in the presence of a cation is expected. Also shift in the chemical shifts of ^{13}C NMR

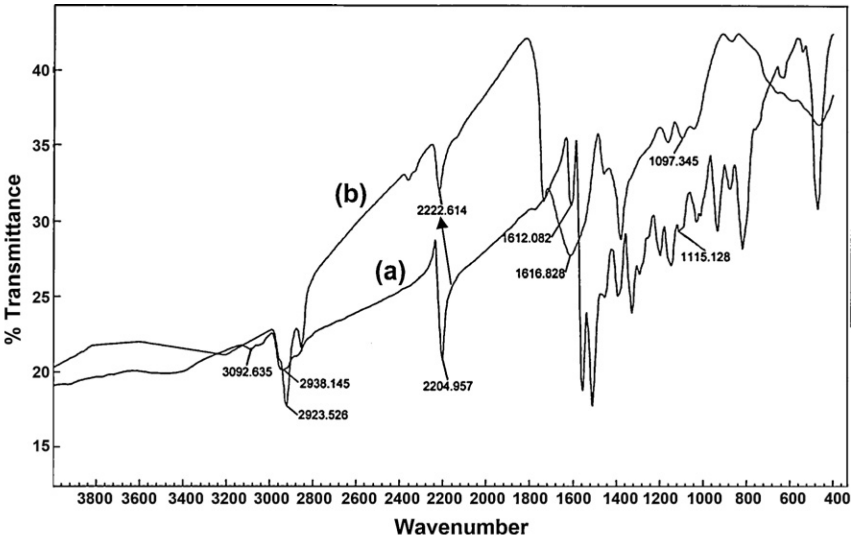

Fig. 7. IR-spectra of **2** (a) and its Cu-complex (b).

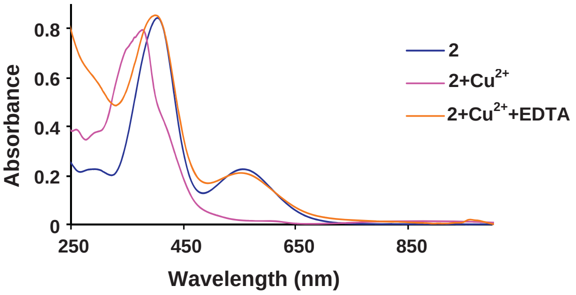

Fig. 8. Absorption spectra of **2** (2.8×10^{-5} M, in CH_3CN) before and after addition of Cu^{2+} solution (4.28×10^{-5} M, in H_2O) and reversal of change upon addition of EDTA solution.

signals, associated with the carbon atoms of cyclopentadienyl ring [18] and/or the olefin bridge is expected. The disappearance of low energy band at 557 nm of **2**, accompanied by the appearance of a new band at 871 nm, in the presence of Cu^{2+}, in our investigation is in good agreement with the proposed interaction. Though, the NMR studies did not reveal any significant information owing to the paramagnetic nature of Cu^{2+}, the UV–vis observations, as explained in Section 3.2 revealed a high energy shift of π–π^* transition (406 → 379 nm), due to the disturbance in the π-conjugation. This observation is further supplemented by a high energy shift from 2204.957 cm^{-1} to 2222.614 cm^{-1} (Fig. 7) of the ν(CN) band of **2** in the complex [**2**:Cu^{2+}], which also rules out the involvement of cyano groups of dicyanovinyl group in binding with copper. On the basis of these observations, it appears that the sensing mechanism for Cu^{2+} involves both types of interactions, i.e. the interaction of Cu^{2+} with both the d-electrons of ferrocene as well as π-electron system of the chromophore, constituting a unique example. The above proposed binding model of Cu^{2+} with **2** is shown in Scheme 2.

The reversibility of the cation sensing process was checked by the addition of EDTA solution to a solution of the complex [**2**:Cu^{2+}], which resulted in the reversal of the original absorption spectrum indicating the quenching of Cu^{2+} (Fig. 8).

4. Practical application

The sensing of Cu^{2+} by **2** also worked on solid support. Thus when silica gel (60–120 mesh, 1.0 g, colorless) was soaked in **2** (in CH_3CN, 5 mL, 1×10^{-3} M) and solvent removed, dark olive color was imparted to silica (Fig. 9). When it was treated with 5 mL aqueous solutions of Cu^{2+} at three different concentrations (0.1 M, 0.01 M and 0.001 M), the dark olive color promptly turned greenish yellow, pale yellow and light olive, respectively. Solvent was removed under reduced pressure and the obtained colored silica was dried in oven. Since the color change was clearly detected, the sensor **2** can be used for practical applications.

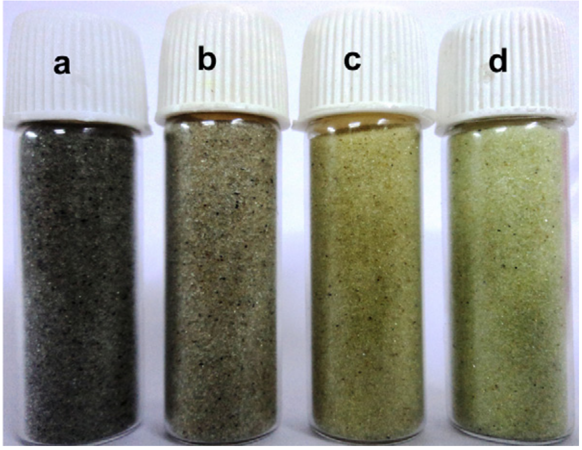

Fig. 9. Changes in color of **2** in the solid state upon addition of aqueous solutions of Cu^{2+}: (a) **2** (1.0×10^{-3} M, in CH_3CN), (b) **2** + 0.001 M Cu^{2+}, (c) **2** + 0.01 M Cu^{2+}, (d) **2** + 0.1 M Cu^{2+}.

5. Conclusion

In summary, we have synthesized a new ferrocenyl derivative **2**, exhibiting intramolecular charge-transfer which gets disturbed by the presence of Cu^{2+}. This perturbation is manifested in terms of absorption as well as electrochemical changes suggesting **2** to be a dual signaling chemosensor for Cu^{2+}. Absorption spectra associated with the color change, allow the 'naked-eye' detection in solution as well as when supported on silica. The sensing event has been proposed to proceed via the interaction of Cu^{2+} with d-electrons as well as the π-electron system of **2**.

Acknowledgements

PK and KS are thankful to CSIR [01(2265)/08-EMR(II)], New Delhi for financial assistance. MK is grateful to UGC, New Delhi for junior research fellowship. KS thanks DST, New Delhi for the research grant SR/SI/OC-27/2009.

Appendix A. Supplementary data

Supplementary data associated with this article can be found, in the online version, at doi:10.1016/j.talanta.2011.05.026.

References

[1] (a) C. Andreini, L. Banci, I. Bertini, A. Rosato, J. Proteome Res. 7 (2008) 209–216;
(b) E.L. Que, D.W. Domaille, C.J. Chang, Chem. Rev. 108 (2008) 1517–1549;
(c) E.D. Harris, J. Trace, Elem. Exp. Med. 14 (2001) 207–210;
(d) M.C. Linder, M. Hazegh-Azam, Am. J. Clin. Nutr. 63 (1996) 797S–811S;
(e) R. Uauy, M. Olivares, M. Gonzalez, Am. J. Clin. Nutr. 67 (1998) 952S–959S.
[2] (a) A.K. Jain, R.K. Singh, S. Jain, J. Raisoni, Transit. Met. Chem. 33 (2008) 243–249;
(b) S.L. Belli, A. Zirino, Anal. Chem. 65 (1993) 2583–2589.
[3] K.L. Ciesienski, L.M. Hyman, S. Derisavifard, K.J. Franz, Inorg. Chem. 49 (2010) 6808–6810.
[4] M. Lin, M. Cho, W. Choe, Y. Son, Y. Lee, Electrochim. Acta 54 (2009) 7012–7017.
[5] (a) P.D. Beer, Chem. Soc. Rev. 18 (1989) 409–450;
(b) P.D. Beer, P.A. Gale, G.Z. Chen, Coord. Chem. Rev. 185–186 (1999) 3–36;
(c) P.D. Beer, P.A. Gale, G.Z. Chen, J. Chem. Soc., Dalton Trans. (1999) 1897–1909.
[6] (a) F. Zapata, A. Caballero, A. Espinosa, A. Tarraga, P. Molina, Inorg. Chem. 48 (2009) 11566–11575;
(b) F. Zapata, A. Caballero, A. Espinosa, A. Tarraga, P. Molina, J. Org. Chem. 73 (2008) 4034–4044;
(c) F. Zapata, A. Caballero, A. Tarraga, P. Molina, J. Org. Chem. 75 (2010) 162–169;
(d) F. Zapata, A. Caballero, A. Espinosa, A. Tarraga, P. Molina, J. Org. Chem. 74 (2009) 4787–4796.
[7] P. Molina, A. Tarraga, A. Caballero, Eur. J. Inorg. Chem. (2008) 3401–3417.
[8] S. Fery-Forgues, B. Delavaux-Nicot, J. Photochem. Photobiol. A: Chem. 132 (2000) 137–159.
[9] (a) P. Kaur, S. Kaur, K. Singh, Tetrahedron Lett. 48 (2007) 7191–7193;
(b) P. Kaur, S. Kaur, A. Mahajan, K. Singh, Inorg. Chem. Commun. 11 (2008) 626–629;
(c) P. Kaur, S. Kaur, K. Singh, Inorg. Chem. Commun. 12 (2009) 978–981;
(d) P. Kaur, D. Sareen, S. Kaur, K. Singh, Inorg. Chem. Commun. 12 (2009) 272–275;
(e) P. Kaur, D. Sareen, Dyes Pigm. 88 (2011) 296–300;
(f) P. Kaur, S. Kaur, Y. Kasetti, P.V. Bharatam, K. Singh, Talanta 83 (2010) 644–650;
(g) P. Kaur, D. Sareen, K. Singh, Talanta 83 (2011) 1695–1700;
(h) P. Kaur, S. Kaur, K. Singh, Talanta 84 (2011) 947–951.
[10] L. Chen, G. Qian, Y. Cui, X. Jin, Z. Wang, M. Wang, J. Phys. Chem. B 110 (2006) 19176–19182.
[11] T. Farrel, T. Meyer-Friedrichsen, M. Malessa, D. Haase, W. Saak, I. Asselberghs, K. Wostyn, K. Caliz, A. Persoons, J. Heck, A.R. Manning, J. Chem. Soc., Dalton Trans. (2001) 29–36, and references cited therein.
[12] (a) S. Barlow, H.E. Bunting, C. Ringham, J.C. Green, G.U. Bublitz, S.G. Boxer, J.W. Perry, S.R. Marder, J. Am. Chem. Soc. 121 (1999) 3715–3723;

(b) Y.S. Sohn, D.N. Hendrickson, H.B. Gray, J. Am. Chem. Soc. 93 (1971) 3603–3612.

[13] V. Lloveras, A. Caballero, A. Tarraga, M.D. Velasco, A. Espinosa, K. Wurst, D.J. Evans, J. Vidal-Gancedo, C. Rovira, P. Molina, J. Veciana, Eur. J. Inorg. Chem. (2005) 2436–2450.

[14] P. Gans, A. Sabatini, A. Vacca, Talanta 43 (1996) 1739–1753.

[15] Detection limit (DL) is given as DL = (0.03 × RSDB), (χ_A/c_0), where RSDB (relative standard deviation of the background expressed as a percent) is the sensitivity (the slope of the calibration curve of intensity versus composition), χ_A is the net analyte signal (i.e. signal above background) and c_0 is the composition of the element in the sample.

[16] S.M. Batterjee, M.I. Marzouk, M.E. Aazab, M.A. El-Hashash, Appl. Organometal. Chem. 17 (2003) 291–297.

[17] J.C. Medina, T.T. Goodnow, M.T. Rojas, J.L. Atwood, B.C. Lynn, A.E. Kaifer, G.W. Gokel, J. Am. Chem. Soc. 114 (1992) 10583–10595.

[18] M.C. Grossel, D.G. Hamilton, J.I. Fuller, E.M. Barios, J. Chem. Soc., Dalton Trans. (1997) 3471–3477.

[19] F.A. Cotton, G. Wilkinson, Advanced Inorganic Chemistry, 5th edition, Wiley Interscience, New York, 1988.